

Supporting Information

Measuring Size Dependence of Thermal Conductivity of Suspended Graphene Disks Using Null-Point Scanning Thermal Microscopy

*Gwangseok Hwang, Ohmyoung Kwon**

School of Mechanical Engineering, Korea University, Seoul 136-701, Korea

* E-mail: omkwon@korea.ac.kr

Table of Contents

1. Fabrication of suspended CVD-grown graphene disks
2. Determination of maximum allowable T_c at which NP SThM remains valid
3. Profiles of φ and undisturbed temperature for 10 suspended graphene disks with radii of 50–3680 nm
4. Estimation of radius of tip–sample thermal contact
5. Estimation of R_p of SThM probe

This material is available free of charge via the Internet at <http://pubs.acs.org>.

1. Fabrication of suspended CVD-grown graphene disks

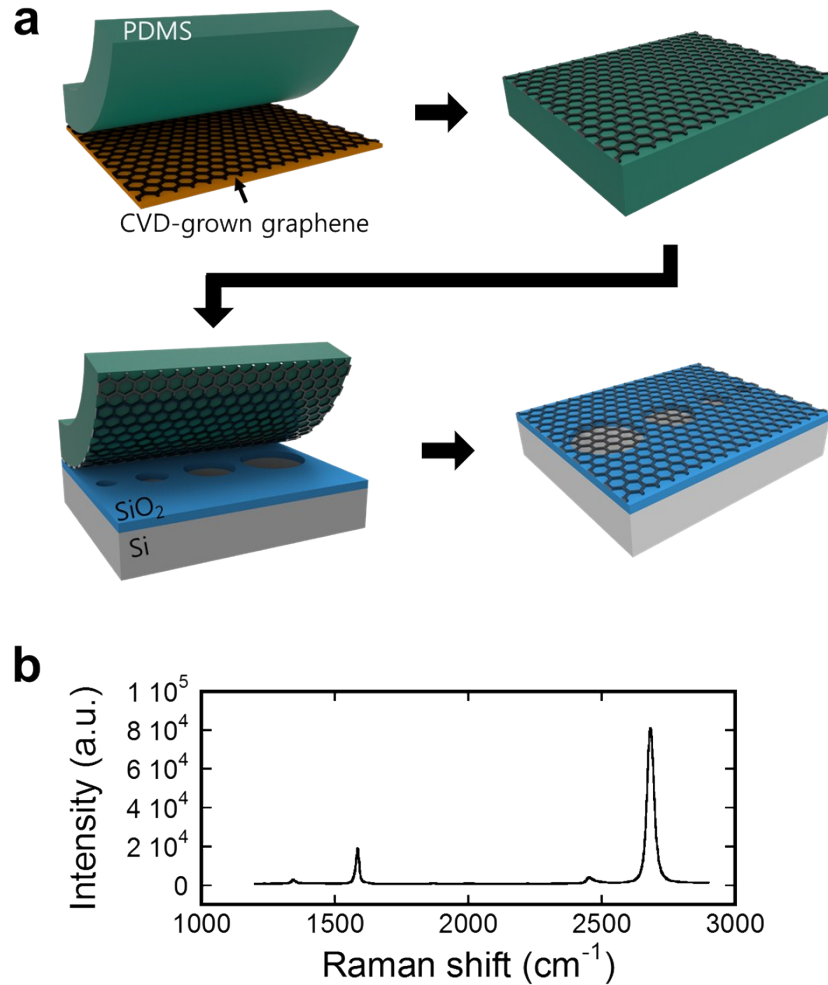


Figure S1. (a) Transfer process of CVD-grown graphene onto prefabricated substrate with PDMS stamping method. (b) Raman spectra obtained at an arbitrary location of CVD-grown graphene transferred to SiO₂ (100 nm)/Si substrate.

Figure S1a illustrates the fabrication process of the sample used in the experiment. First, graphene was grown on copper foil by chemical vapor deposition (CVD), and polydimethylsiloxane (PDMS) was attached to it. Then, fabrication of the PDMS/graphene stamp was completed by wet-etching of the copper foil. In parallel, a hole-patterned SiO₂ (100

nm)/Si substrate with hole radii of 50–3680 nm was fabricated by standard e-beam lithography, photolithography, and reactive ion etching. We obtained the suspended graphene disks by stamping the PDMS/graphene stamp on the hole-patterned SiO₂/Si substrate.

The quality of the CVD-grown graphene was checked by Raman spectroscopy. As shown in Figure S1b, the negligible D peak implies that the graphene was residue-free, and the amplitude of the G peak was four times larger than that of the 2D peak, which indicates that the graphene was a monolayer.

2. Determination of maximum allowable T_c at which NP SThM remains valid

As noted in the main manuscript, to improve the signal-to-noise ratio of NP SThM, we maximized the difference between the temperature jumps (i.e., $T_{j1} - T_{j2}$). However, as shown in eq 8, if φ changes because of the variation in R_c owing to excessive heating of the probe, NP SThM is no longer valid. Therefore, we determined the heating conditions for the thermocouple junction of the SThM probe under which φ does not change and NP SThM remains valid.

We measured T_c and T_{nc} at the center of a suspended graphene disk with a radius of 1.56 μm while heating the thermocouple junction of the probe from about 30 to 105 °C. To check the maximum allowable heating temperature at which φ remains unchanged, as shown in Figure S2, we observed the slope of T_c with respect to T_j . This corresponds to φ , as shown in eq 8. Figure S2 shows that the linearity was experimentally verified to break down when T_c exceeded 90 °C. In other words, φ was no longer constant when T_c exceeded about 90 °C. Therefore, we performed NP SThM on all of the suspended graphene disks while ensuring that T_c stayed below 80 °C during the measurement.

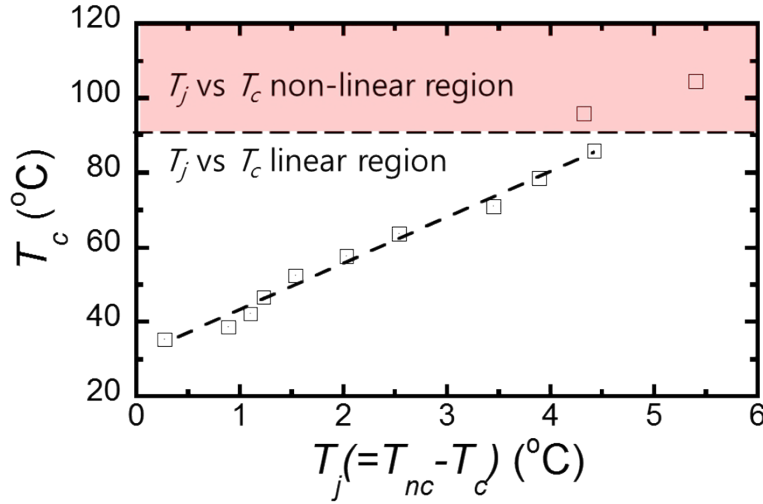


Figure S2. T_c represented as function of $T_j (= T_{nc} - T_c)$ measured at several different probe tip temperatures ranging from about 30 to 105 °C. The data were measured at the center of a suspended CVD-grown graphene disk with a radius of 1.56 μm . The slope of T_c with respect to T_j corresponds to ϕ . The linearity between T_j and T_c broke down when T_c exceeded 90 °C.

3. Profiles of ϕ and undisturbed temperature for 10 suspended graphene disks with radii of 50–3680 nm

Figure S3 shows the profiles of ϕ and the undisturbed temperature, which were calculated by substituting the measured data (T_{c1} , T_{nc1} , T_{c2} , and T_{nc2}) into eqs 8 and 9 for 10 suspended graphene disks with radii of 50–3680 nm. By checking that the undisturbed temperature obtained by NP SThM remained constant at room temperature across the entire scanning line, we confirmed the reliability of the ϕ data obtained simultaneously with the undisturbed temperature for all 10 graphene disks.

For the five relatively large graphene disks ($D/2 = 3.68, 2.70, 2.16, 1.56,$ and $0.45 \mu\text{m}$), whose ϕ profiles are shown in Figure S2a–e, ϕ stayed almost constant in the supported region.

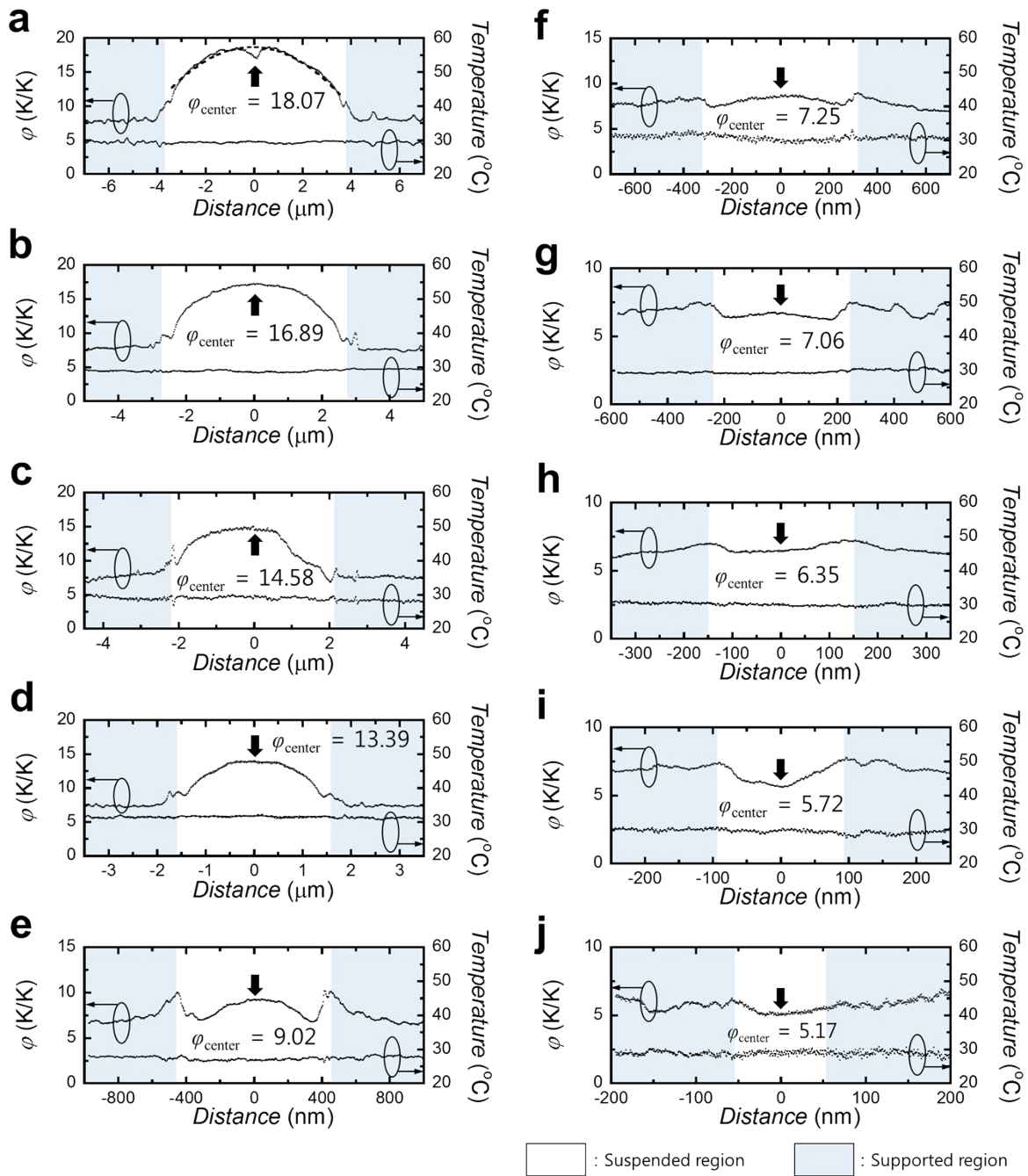


Figure S3. Profiles of ϕ and undisturbed temperature calculated by substituting measured data (T_{c1} , T_{nc1} , T_{c2} , and T_{nc2}) into eqs 8 and 9 for 10 suspended CVD-grown graphene disks with radii of 50–3680 nm: (a) $D/2 = 3.68 \mu\text{m}$, (b) $D/2 = 2.70 \mu\text{m}$, (c) $D/2 = 2.16 \mu\text{m}$, (d) $D/2 = 1.56 \mu\text{m}$, (e) $D/2 = 450 \text{ nm}$, (f) $D/2 = 340 \text{ nm}$, (g) $D/2 = 250 \text{ nm}$, (h) $D/2 = 150 \text{ nm}$, (i) $D/2 = 90 \text{ nm}$, (j) $D/2 = 50 \text{ nm}$.

Then, after showing an abrupt N-shaped change at the edge of the suspended region, it increased gradually beginning at the edge of the suspended disk, peaked at the center of the disk, and then decreased. The abrupt N-shaped change at the edge of the suspended region seemed to be caused by the abrupt change in the tip–sample thermal contact area due to the sharp topographic change at the edge.

However, for the five smaller disks ($D/2 = 340, 250, 150, 90,$ and 50 nm), whose φ profiles are shown in Figure S2f–j, the change in φ observed at the edge of the disk gradually became smooth. The reason seems to be that the topographic change at the edge became rather smooth with decreasing hole size, as shown in Figure 3d.

For the three smallest graphene disks ($D/2 = 150, 90,$ and 50 nm), whose φ profiles are shown in Figure S2h–j, unlike the behavior of φ for the larger disks, φ decreased as the tip of the probe approached the center of the suspended region. This unique behavior of φ for the smallest disks is explained in the main text.

To observe the variation in R_s with respect to the size of the graphene disk, we extracted φ at the center of the disk (φ_{center}) from the measured φ profiles for the 10 suspended graphene disks in Figure S3; Figure 4 in the main manuscript summarizes φ_{center} as a function of $\ln(D/2a)$. For the graphene disk with a radius of $3.68 \mu\text{m}$ (Figure S3a), we extracted φ_{center} by using polynomial fitting of φ in the suspended region. Because of some nonphysical disturbances to the topography, the φ profile near the center of the disk was distorted.

4. Estimation of radius of tip–sample thermal contact

We estimated the radius of the tip–sample thermal contact area on the supported graphene (a_{sup}) as follows:^{S1}

$$a_{\text{sup}} = 2.08 \sqrt{\frac{r_{\text{tip}} \cos \theta}{\ln \psi}} \quad (\text{S1})$$

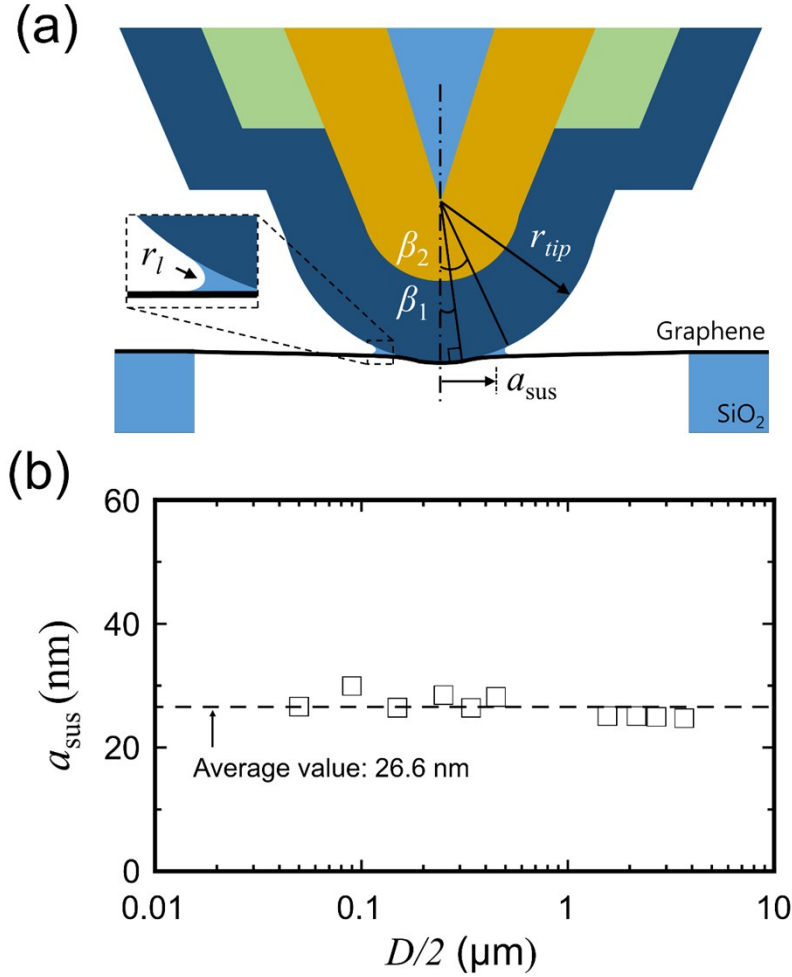


Figure S4. (a) Schematic of cross section of SThM tip in contact with suspended graphene disk. a_{sus} is the radius of the tip–sample thermal contact, β_1 is the angle between the central axis of the tip and a line perpendicular to the tangent of the graphene and the tip, and β_2 is the angle from the central axis of the tip to the edge of the liquid film. (b) a_{sus} calculated from the experimental data at each disk radius.

where r_{tip} is the radius of the probe tip, θ is the water contact angle, and ψ is the relative humidity. The radius of the tip used in the experiment was about 100 nm, the water contact angle

on the graphene was 33.2° ,^{S2} and the relative humidity during the experiment was about 50%. By substituting these values into eq S1, a_{sup} was calculated as 23 nm.

At the center of the suspended graphene disk, the radius of the tip–sample thermal contact (a_{sus}) increases slightly because of the change in the surface topography, as illustrated in Figure S4a, where β_1 is the angle between the central axis of the tip and a line perpendicular to the tangent of the graphene and the tip, and β_2 is the angle from the central axis of the tip to the edge of the liquid film. As shown by Figure S4a, β_1 can be calculated from the radius of the graphene disk and the dip depth of the probe at the center of the disk. Once β_1 is calculated, β_2 can be obtained from^{S1}

$$\cos \beta_2 = \cos \beta_1 - \frac{2r_l}{r_{\text{tip}}} \quad (\text{S2})$$

where $r_l = -1.08/\ln\psi$ is the radius of the liquid film that exists between the tip and the graphene.^{S1} Finally, from simple geometry a_{sus} can be obtained as

$$a_{\text{sus}} = r_{\text{tip}} \sin \beta_2 \quad (\text{S3})$$

Figure S4b shows the values of a_{sus} calculated from the experimental data with respect to the radius of the disk. We used the average of a_{sus} in the main text. As shown in Figure S4b, a_{sus} is almost constant. However, for the smaller disks, the values of a_{sus} are slightly scattered. The biggest deviation was 3.3 nm.

5. Estimation of R_p of SThM probe

In this study, we obtained R_p by analyzing the governing equation for T_j ($= T_c - T_{\text{nc}}$), which is the temperature jump in the probe owing to heat flux through the tip–sample thermal

contact. In a previous study, Kim et al. obtained the governing equation and boundary conditions for T_j by subtracting the governing equation and boundary conditions for T_{nc} from those of T_c ^{S4}:

$$\frac{d}{d\xi} \left[\sum A_i(\xi) k_i \frac{dT_j(\xi)}{d\xi} \right] - [p(\xi) h_{eff}(\xi) + p_\infty(\xi) h_\infty(\xi)] T_j(\xi) = 0 \quad (S4)$$

$$\sum A_i k_i \frac{dT_j(0)}{d\xi} = Q_{st}, \quad T_j(L) = 0 \quad (S5)$$

where ξ represents the position in the probe ($\xi = 0$ at the end of the tip; $\xi = L$ at the end of the cantilever), A_i is the cross section of the i^{th} layer, k_i is the thermal conductivity of the material composing the i^{th} layer, p is the perimeter of the probe related to the surface that exchanges heat flux with the sample surface, h_{eff} is the effective heat transfer coefficient between the probe and the sample, p_∞ is the perimeter of the probe related to the surface that exchanges heat flux with the surroundings excluding the sample, h_∞ is the effective heat transfer coefficient between the probe and the surroundings excluding the sample, and Q_{st} is the heat flux from the sample to the tip through the tip–sample thermal contact.

Hence, R_p defined by eq 2 in the main text is the same as $T_j(\xi_{tc})/Q_{st}$, where ξ_{tc} is the position of the thermocouple junction. By substituting the specifications of the SThM probe used in this study into eqs (S4) and (S5) and then solving the equations, we obtained a value of 0.258 K/ μ W for R_p .

References

- S1. K. Luo, Z. Shi, J. Varesi, A. Majumdar, *J. Vac. Sci. Technol., B* 1997, **15**, 349.
- S2. J. Rafiee, X. Mi, H. Gullapalli, A. V. Thomas, F. Yavari, Y. Shi, P. M. Ajayan, N. A. Koratkar, *Nat. Mater.*, 2012, **11**, 217–222.
- S3. G. Hwang, J. Chung, O. Kwon, *Rev. Sci. Instrum.*, 2014, **85**, 114901.
- S4. K. Kim, J. Chung, G. Hwang, O. Kwon, J. S. Lee, *ACS Nano*, 2011, **5**, 8700–8709.